Author Manuscript

Author Manuscript

Author Manuscript

Author Manuscript

HHS Public Access

Author manuscript

Dev Dyn. Author manuscript; available in PMC 2019 November 07.

Published in final edited form as:

Dev Dyn. 2018 November ; 247(11): 1227–1236. doi:10.1002/dvdy.24675.

Comparative Analysis of cul5 and rbx2 Expression in the Developing and Adult Murine Brain and Their Essentiality During Mouse Embryogenesis

Keiko Hino[1], **Sergi Simó**[1,*], and **Jonathan A. Cooper**[2]

[1]Department of Cell Biology and Human Anatomy, University of California, Davis, California

[2]Division of Basic Sciences, Fred Hutchinson Cancer Research Center, Seattle, Washington

Abstract

Background: The E3 Cullin 5-RING ubiquitin ligase (CRL5) is a multiprotein complex that has recently been highlighted as a major regulator of central nervous system development. Cullin 5 (Cul5) and the RING finger protein Rbx2 are two CRL5 core components required for CRL5 function in the brain, but their full expression patterns and developmental functions have not been described in detail.

Results: Using a gene-trap mouse model for Cul5 and a knock-in-knockout mouse model for Rbx2, we show that lack of Cul5, but not Rbx2, disrupts blastocyst formation. However, Rbx2 is required for embryo survival at later embryonic stages. We also show that cul5 is expressed in the embryo proper as early as E7.5 and its expression is mostly restricted to the central nervous system and limbs at later time points. Finally, we show that rbx2 and cul5 are co-expressed in most areas of the brain during development and in the adult.

Conclusions: Our results show that Cul5, but not Rbx2, is required during early embryogenesis and suggests that Cul5 has Rbx2-independent functions in early development. In the brain, Cul5 and Rbx2 are expressed in a similar fashion, allowing the nucleation of an active CRL5 complex.

Keywords

Embryogenesis; brain development; CRL5; *cul5*; *rbx2*

Introduction

Cullin-RING ligases (CRLs) constitute a subfamily of E3 ubiquitin ligases with a common mechanism of assembly and regulation. Each CRL is a multiprotein complex with a Cullin protein as a backbone (Petroski and Deshaies, 2005). There are seven Cullins in vertebrates: Cul1, −2, −3, −4A, 4B, −5, and −7. The C terminus of the Cullin binds to a RING finger protein, either Rbx1/Roc1 or Rbx2/Rnf7/Sag1, which transfers the small ubiquitin-like protein Nedd8 to the Cullin. Neddylation stimulates ubiquitin transfer by the Cullin-Rbx

*Correspondence to: Sergi Simó, University of California, Davis, One Shields Avenue, 3403 Tupper Hall, Davis, CA 95616. ssimo@ucdavis.edu.

Additional supporting information may be found in the online version of this article.

Author Manuscript Author Manuscript Author Manuscript Author Manuscript

complex, utilizing the same Rbx protein to bind the ubiquitin E2 enzyme that donates ubiquitin to substrates (Huang et al., 2009). The N terminus of the Cullin binds through linker proteins to substrate-specific adaptor proteins. The large number of substrate adaptors, more than 500 in vertebrates, makes CRLs the most abundant subfamily of E3 ubiquitin ligases (Petroski and Deshaies, 2005).

Cul5 is a relatively recently evolved member of the Cullin family, being restricted to metazoans (Sarikas et al., 2011). Unlike other Cullins, Cul5 principally binds Rbx2 to generate an active CRL5 complex, although Rbx1 can also be recruited in particular cases (Dentice et al., 2005; Mahrour et al., 2008; Huang et al., 2009; Wang et al., 2015). Cul5 recruits, directly or indirectly, substrates to be polyubiquitylated through one of its substrate adaptor proteins, numbering 38 in vertebrates, thereby allowing regulation of a large variety of protein substrates (Okumura et al., 2016). Accordingly, CRL5 has been implicated in immunity, cell cycle, cell migration, viral replication, and cancer development/progression (Laszlo and Cooper, 2009; Teckchandani et al., 2014; Okumura et al., 2016). Recently, Cul5 and Rbx2 have also been shown to be crucial during central nervous system (CNS) development, regulating both neuronal migration and neuron position (Feng et al., 2007; Simo et al., 2010; Simo and Cooper, 2013; Moon et al., 2015; Fairchild et al., 2018). Moreover, Rbx2 genetrap (GT) mice die prenatally (at embryonic day E11.5–12.5) due to vascularization defects (Tan et al., 2012).

Given the prominent role of Cul5 and Rbx2 in CNS development, we sought to understand the expression pattern of *cul5* and *rbx2* during brain development and in the adult. Here, we describe the generation of Cul5 and Rbx2 GT mutant mice that express the ß-galactoside (ß-Gal) enzyme under the control of the endogenous Cul5/Rbx2 locus, respectively. We also determine Cul5 expression in mid-embryogenesis and compare Cul5 and Rbx2 expression patterns during brain development and in the adult. Furthermore, we provide evidence that, whereas Rbx2 is not required, Cul5 is essential for blastocyst formation, indicating that Cul5 has Rbx2-independent functions during early embryogenesis.

Results

cul5 but not *rbx2* is an Essential Gene at Preimplantation Stages

To analyze the expression and essentiality of cul5 and *rbx2* during development, we obtained mouse GT lines of *cul5* and *rbx2*, both in chromosome 9. The *cul5GT* was generated by random integration of a cassette containing approximately 1.5 kb of intron 1 and the acceptor splice site of mouse *engrailed2* (En2), followed by ß-galactosidase fused with neomycin transferase (ß-geo) and a polyadenylation signal (pA). This insertion disrupts the first intron of the *cul5* gene (Fig. 1A). The *rbx2GT* was generated in mouse embryonic stem cells (mESCs) by homologous recombination. Intron 1 of *rbx2* contains, in order, an FRT site, the splicing acceptor of En2, ß-geo, a pA cassette, an FRT site, and a LoxP site. A second LoxP site was inserted in exon 2 (Fig. 1B; *rbx2GT* allele). mESCs from both strains were used to generate chimeric mice, which were bred to obtain heterozygous animals. The presence of the insert was verified by PCR genotyping in each case.

Author Manuscript Author Manuscript Author Manuscript Author Manuscript

Interestingly, when heterozygous *cul5GT* mice were bred, no homozygous pups were obtained (Chi-square test $P = 0.00055$) (Fig. 1C). To determine whether Cul5 was necessary during early or late embryogenesis, we collected blastocysts from the uterine lumen at E3.5. No homozygous mutant blastocysts were recovered (Chi-square test $P = 0.00041$) (Fig. 1C), indicating that Cul5 is essential during early, preimplantation embryogenesis. It is important to note that the lack of homozygous mutants is not a consequence of progenitor sterility or defects in gamete production, as the *cul5*GT allele could be successfully transmitted from heterozygous *cul5*GT male or female mice (data not shown). Given that Cul5 recruits Rbx2 to form a functional CRL5 complex in the CNS (Simo and Cooper, 2013; Fairchild et al., 2018), we tested whether *rbx2* was also necessary during early embryogenesis. We mated rbx2GT mice first with FLPeR mice and then with Meox2-Cre to generate the *rbx2* knockout (KO) allele (Fig. 1B) (Farley et al., 2000; Tallquist and Soriano, 2000). Absence of rbx2 exon 2 (rbx2KO) was verified by PCR genotyping. Similar to *cul5GT*, no rbx2 mutant pups (postnatal day P0) were recovered from heterozygous *rbx2*KO intercrossing (Chi-square test $P = 0.00228$) (Fig. 1D). However, we were able to recover rbx2 −/− blastocysts, although in lower numbers than the expected ratio (Chi-square test $P = 0.00012$) (Fig. 1D). These results indicate that Cul5, but not Rbx2, is essential for preimplantation development.

cul5 Expression During Mid-gestation and in the Central Nervous System

Cul5 GT heterozygous mice express ß-geo under the control of the endogenous *cul5* locus. We used x-Gal staining to assess ß-geo expression during development and in adulthood. In toto x-Gal staining of E7.5 embryos revealed intense expression of *cul5* in the embryo proper, whereas lower *cul5* expression was observed in the extra-embryonic body (Fig. 2A). At E9.5, the highest expression was detected in the future CNS, the limb buds, and the mandibular compartment of the first branchial arch (Fig. 2B). In the cephalic region, there is a high expression of *cul5* in the neuroepithelium surrounding the telencephalic vesicle and the III ventricle, and more caudally there is also high expression in the neural tube (Fig. 2B). At E11.5, *cul5* is similarly expressed at the highest level in the CNS, forelimbs, and hindlimbs. It is interesting to note that at this stage *cul5* was expressed distinctively at the eye compartment, which contains the lenses, pigmented epithelia, and early neural retina (Fig. 2C). Expression of *cul5* in the retina correlates with *rbx2* expression (Fairchild et al., 2018). Depletion of Rbx2 in the retina disrupts retinal neuron position in a SOCS7-dependent and -independent fashion (Fairchild et al., 2018). The facts that 1) Cul5, Rbx2, and SOCS7 are expressed in the retina and 2) absence of Rbx2 or SOCS7 disrupts retinal neuron positioning suggests an active CRL5 complex regulates retina morphogenesis.

From E14.5 onward, we restricted our analysis to the developing brain. In the olfactory bulb, *cul5* expression increased throughout development with the highest expression during adulthood (Fig. 3A, Table S1). At E14.5, there was strong expression in the mitral cell layer, which was maintained and increased during development (Fig. 3A). Expression of *cul5* was also detected in the olfactory bulb granule cell layer at postnatal stages, which correlates with granule cell genesis (Bayer, 1983). Similarly, expression of *cul5* in the glomerular cell layer also increased markedly during development, achieving the highest expression in the adult. There was little or no signal in the subependymal zone in the postnatal and adult olfactory bulb, suggesting that *cul5* expression in adult-born interneurons of the olfactory

Author Manuscript Author Manuscript Author Manuscript Author Manuscript

bulb is induced when these neurons reach the olfactory bulb and is absent during migration to the olfactory bulb through the rostral migratory stream (Lledo et al., 2008).

In the neocortex, Cul5 expression was detected at least from E14.5 (Fig. 3B, Table 1), and high *cul5* expression in the cortical plate was observed from E16.5 until adulthood, when we were able to detect the highest expression. Also, high expression was detected in the subplate during development and in early post-natal stages (Fig. 3B,D) (Torres-Reveron and Friedlander, 2007). Overall, the strongest expression in the forebrain was found in the piriform cortex (Fig. 3D). Moreover, LacZ staining in other areas of the neocortex including the cingular-retrosplenial cor-tex and the frontal, parietal, and temporal zones of the neocor-tex was also observed.

Little *cul5* expression was detected in the primordium of the hippocampus at E14.5, although by E16.5 expression increased significantly in the ventricular zone (VZ) and pyramidal cells (Fig. 3C). Later on, from P0 to adult, expression was higher in the Cornus Ammonis CA1 than the CA3. *Cul5* was not expressed in the primordium of the dentate gyrus during embryonic stages, but signal started to develop in granule cells after birth, reaching the maximum levels in the adult. It is interesting to note that *cul5* was also expressed in proliferative areas of the hippocampus during development and in the adult (Fig. 3C). At E16.5, *cul5* expression could be detected in the ventricular zone of the hippocampus and the dentate neuroepithelium, which produces pools of undifferentiated precursors that migrate and give rise to the dentate gyrus (Khalaf-Nazzal and Francis, 2013). In the adult, *cul5* expression was enriched in the subgranular zone of the dentate gyrus, which is known to be a neurogenic area in the adult CNS (Fig. 3C).

In some areas of the forebrain, such as the amygdala complex, tenia tecta, and dorsolateral septum, *cul5* was also expressed strongly during development and in the adult. By contrast, the expression of *cul5* in the accumbens nucleus or the medial septum was developmentally up-regulated (Table 1, Fig. 3D). The striatum showed a moderate-high expression in the caudateputamen during embryonic and early postnatal stages that decreased in the adult. Conversely, the globus pallidus showed a weak signal that increased slightly during development even though it remained faint in the adult. In the diencephalon, the subcommissural organ and the medial habenula of the epithalamus expressed *cul5* strongly (Table 1, Fig. 3D). Expression in the habenula decreased slightly during development.

In the thalamus, *cul5* was detected in all nuclei, especially at E18.5. An interesting expression pattern was detected in the lateral geniculate nuclei, where *cul5* reached an expression peak by E18.5, the signal was not detected at P0, and then *cul5* expression was recovered in the adult (Table 1). In the hypothalamus, *cul5* expression was low in the majority of nuclei at E14.5 but increased by E16.5 and was sustained through to adult hood.

In the mesencephalon, *cul5* was ubiquitously expressed, with the strongest signal in the periaqueductal gray area during embryonic stages. The superior and the inferior colliculus, the substantia nigra, and the dorsal raphe showed moderate Cul5 expression from E14.5 until adulthood (Table 1). In the hindbrain, *culS* was expressed at E11.5 in the rhombic lip (Fig. 2E). At E14.5, *culS* expression is observed in the lateral/caudal side of the rhombic lip.

Author Manuscript Author Manuscript Author Manuscript Author Manuscript

This moderate expression of Cul5 in the rhombic lip is maintained between E14.5 and E16.5 (Table 1). Purkinje cells showed strong LacZ staining during development and in the adult (Fig. 4A,B). Also, a subset of cells in the adult molecular layer and internal granular layer showed high *culS* expression (Fig. 4B). Based on their position, these cells resemble the distribution of GABAergic interneurons in the adult cerebellum. On the contrary, expression of cul5 in cerebellar granule increases over time (Table 1). Initially, granule cell precursors in the external granular layer expressed low levels of *culS* at all stages (Fig. 4A,B). Expression increased when mature granule cells migrated inward to form the internal granular layer in at P5 and increased further in the adult (Fig. 4B). *Cul5* was highly expressed in other areas of the hindbrain, such as the pontine nuclei during development and in the adult (Table 1), the inferior olive (Fig. 4C), the area postrema in early postnatal stages (P0–P5) (Fig. 4C), and the cuneate nucleus in the adult (Fig. 4C).

rbx2 Expression in the Central Nervous System

Our previous work indicates that the presence of Rbx2 is necessary for Cul5 stability, suggesting that co-expression of Cul5 and Rbx2, at least in the brain, is necessary for CRL5 function (Simo and Cooper, 2013). We used *rbx2GT* mice to determine *rbx2* expression in the developing and adult brain. As hypothesized based on our previous functional analysis, *rbx2* expression was comparable to *cul5* expression with minor differences (Fig. 5). In the olfactory bulb, *rbx2* was principally expressed in mitral cells, but its expression was also detected in the granule layer of the olfactory bulb at earlier time points (P0) than those of *cul5* (Fig. 5A). In the neocortex, rbx2 was widely expressed but at a seemingly lower level than that of *cul5*. By P0, expression of *rbx2* was homogenous and high in all layers of the neocortex and maintained high through postnatal stages and in the adult (Fig. 5B). The *rbx2* expression pattern in the hippocampus mimics *cul5* (Fig. 5C and Fig. 3C, respectively). No differences in expression patterns were observed in other areas of the developing and adult brain including the diencephalon, cerebellum, and medulla (Fig. 5D,E). Our data indicate that *rbx2* is widely expressed in the developing and adult brain and is comparable, at all stages studied, with *cul5* expression, suggesting that Cul5 and Rbx2 are present in the same areas of the brain and are able to seed a functional CRL5 complex.

Next, we used immunofluorescence to confirm the co-expression of Cul5 and Rbx2 in the brain (Fig. 6). Adult wildtype brains were embedded in paraffin, and consecutive sagittal brain sections were stained with antibodies against Cul5 and Rbx2. Both proteins were ubiquitously detected in the brain with a similar pattern as the x-Gal stainings. High-power images of the cerebellum, hippocampal CA3 and neocortex, and caudate-putamen showed that Cul5 and Rbx2 were expressed in the same cells in different areas of the brain (Fig. 6A–C, respectively). Interestingly, Cul5 and Rbx2 co-expressed in several axon bundles, in particular in the mossy fibers of the hippocampus, where the strongest axonal expression of Cul5 and Rbx2 was detected (Fig. 6B). Our stainings also showed that Cul5 was mostly detected in the cytoplasm, with some nuclear localization particularly in the caudate-putamen (Fig. 6C). Surprisingly, Rbx2 was detected principally in the nucleus of neuronal cells, with less expression detected in the cytoplasm. Finally, we used immunofluorescence to confirm that Cul5 co-expressed with ß-Gal in *rbx2*GT mice. As expected, ubiquitous co-expression of Cul5 and ß-Gal was detected in the brain of rbx2GT adult mice (Fig. 6D–D”’).

Author Manuscript Author Manuscript Author Manuscript Author Manuscript

ß-Gal staining was detected in the cytoplasm with a diffuse signal and bright solid dots, whereas Cul5 was expressed as previously described.

Discussion

In the present study, we aimed to understand the relationship between Cul5 and Rbx2 by analyzing the effects of disrupting the *cul5* and *rbx2* genes on mouse development. We also interrogated the expression patterns of *cul5* during mouse development and compared them to *rbx2* expression, particularly in the CNS. We have found that Cul5 and Rbx2 are both essential for mouse embryonic development (Fig. 1). However, remarkable differences were observed. Intercrossing of heterozygous *cul5*GT mice produced no homozygotes with lethality likely occurring before E3.5 since no homozygous blastocysts were recovered. On the contrary, *rbx2*KO homozygotes were recovered at E3.5, although at a lower ratio than expected, and some mutant *rbx2* embryos were recovered up to E10.5 (data not shown). These data indicate that whereas Cul5 is already essential at preimplantation stages, Rbx2 is not. A previous report showed that *rbx2* homozygous GT embryos survived until E12.5, and at that stage Rbx2 is needed to support Cul1 function (Tan et al., 2012). Despite the strong evidence that Cul5 principally recruits Rbx2 to form a functional CRL5 complex (Kamura et al., 2001; Sasagawa et al., 2007; Huang et al., 2009; Kelsall et al., 2013; Simo and Cooper, 2013), in vitro as well as in vivo experiments suggest that a Cul5-Rbx1 complex is also possible (Kamura et al., 2001; Wang et al., 2015; Onel et al., 2017). Therefore, two possible hypotheses can be proposed to explain the present data: 1) There are RING finger protein (Rbx1/Rbx2)-independent functions for Cul5 during preimplantation stages, or 2) in the absence of Rbx2, Cul5 is able to recruit Rbx1 to establish a partially functional CRL5 complex during early embryogenesis. There are no examples in the literature that indicate that Cullins may function independently of a RING finger protein. Indeed, Rbx2 depletion negatively affects Cul5 expression/stability in neurons (Simo and Cooper, 2013), suggesting that Cul5 requires a RING finger protein for stability and function. Overall, our data suggest that Rbx1 can partially compensate for Rbx2 absence during preimplantation stages. Furthermore, the combination of the expression data presented here with our previous functional analysis suggests that in the CNS *rbx1* may be unable to compensate for *rbx2* in seeding a functional CRL5 complex after mid-gestation.

The preimplantation lethality observed on *cul5*GT intercrossing is remarkable considering that other Cullins tested are not required before implantation: *cull* mutant embryos develop to E6.5 and die afterward with defects in gastrulation; *cul3* die at E7.5 with abnormal gastrulation and defects in extraembryonic structures; different *cul4A* alleles are either viable, with impaired male fertility, or die between E4.5 and 7.5; *cul4B* mutants die by E9.5 with placental defects and developmental delay; and *cul7* mutants are runted, with placental and vascular defects, dying of respiratory distress at birth (Dealy et al., 1999; Singer et al., 1999; Wang et al., 1999; Li et al., 2002; Arai et al., 2003; Kopanja et al., 2011; Jiang et al., 2012). *cul2* mutants have not been studied. *cul5* may be required to coordinate proliferation and differentiation of the zygote into primitive endoderm and inner cell mass before implantation, but this awaits further study.

Author Manuscript Author Manuscript Author Manuscript Author Manuscript

Our detailed description of *cul5* expression in the brain during development and in the adult reveals expression in the nervous system as early as E9.5 (Fig. 2). *cul5* shows a broad and discrete pattern of expression with up-regulation in postnatal stages in granule cells of the olfactory bulb, dentate gyrus, and cerebellum (Table 1). Moreover, *cul5* was expressed in highly proliferative areas such as the ventricular zone of the telencephalon, the subgranular zone of the dentate gyrus, and the rhombic lip; the role of Cul5 in these areas remains to be determined. Our results are in accordance with previous attempts describing *cul5* expression in the adult rodents, although our study provides a more comprehensive and systematic approach (Ceremuga et al., 2001; Ceremuga et al., 2003). A previous study from our lab reported that *cul5* is involved in the control of neuronal migration in the cortical plate (Feng et al., 2007); our results agreed with this possibil-ty according to the strong expression of Cul5 in the cortical plate during development. Our data also show that *cul5* is expressed in the retina at early stages (Fig. 2E). It is interesting to note that a recent study shows *rbx2* is expressed in the retina and, most likely through CRL5 function, is required for proper retina morphogenesis and function (Fairchild et al., 2018). Our comparative expression analysis indicates that *rbx2* expression mimics that of *cul5*. These pieces of evidence support our recent work, where we demonstrated that depletion of *cul5* or *rbx2* resulted in the same phenotypes in the neocortex (Simo and Cooper, 2013). Similarly, the co-expression of Cul5 and Rbx2 detected in the Purkinje cells of the cerebellum supports the phenotypes observed in Rbx2 mutant animals, whereas lack of Rbx2 causes Purkinje cell misposition during development (Simo and Cooper, 2013). It is important to note that *cul5* and *rbx2* might exert a broader spectrum of functions in the CNS based on the extensive expression in all the areas of the brain. As an example, the strong Cul5 and Rbx2 expression detected in the mossy fibers supports our current work indicating that Rbx2, and likely Cul5, participates in mossy fiber innervation (Canales et al, in preparation) and further suggests that detailed study of Cul5/Rbx2 expression may reveal novel CRL5 functions in the developing and adult nervous system.

We showed that Cul5 and Rbx2 are co-expressed in most of the cells analyzed (Fig. 6). These results complement the recent single-cell RNA sequencing studies where *cul5* and *rbx2* are co-expressed in most neuronal and non-neuronal cell populations in the brain (Saunders et al., 2018; Zeisel et al., 2018). Our data also indicate that despite Cul5 and Rbx2 being expressed in the same cells, their subcellular localization is, in general, different, with Cul5 mostly detected in the cytoplasm and Rbx2 mostly detected in the nucleus. Accordingly, Cul5 has been postulated to regulate cellular growth when localized in the nucleus, and preventing nuclear localization disrupts the ability of Cul5 to regulate cellular proliferation, which suggests that Cul5 localization is regulated and important for its function (Willis et al., 2017). Further work will elucidate whether Cul5 and Rbx2 compartmentalization responds to a regulatory control of CRL5 activity or indicates a preference in CRL5 substrate localization.

Author Manuscript Author Manuscript Author Manuscript Author Manuscript

Experimental Procedures

Animals

The *cul5* GT embryonic stem cell clone, AA0096, from International Gene Trap Consortium, was injected into mouse blastocysts and implanted into pseudopregnant females to generate chimeric mice. Chimeric mice were bred to C57BL6 to obtain heterozygotes containing the trapped gene, which were maintained in a mixed 129Sv/C57BL6 strain background. For PCR genotyping we used the following primers (Fig. 1A): primer C, 5'-GTGCAAATGAGGTTG TTCCC-3'; primer WT, 5'-GCCAGCCTGATCCACATAGT-3'; primer GT, 5'-GGCCAAGTTTGTTTCCTTGA-3'. Primer C and primer WT generated an amplicon in the wild-type allele of 650 bp, and primer C and primer GT produced an amplicon in the trapped allele of 850 bp.

The *rbx2* knockout first allele (*rbx2*GT) mouse embryos (Rnf7tm1a(EUCOMM)Wtsi) were obtained from the International Mouse Phenotyping Consortium (IMPC) (Skarnes et al., 2011) and maintained in a mixed 129Sv/C57BL6 strain background. For PCR genotyping of the original GT allele, we used the following primers (Fig. 1B, arrows): primer C, 5'-GTGCCTGTGA TTCCCAAACT-3'; primer WT, 5'-CACGGTTTTACAAGGGCA GT-3'; primer GT, 5'-AAGGGTCGAGAGACAGGTGA-3'. Primer C and primer WT generated an amplicon in the wild-type allele of 373 bp, and primer C and primer GT produced an amplicon in the trapped allele of 671 bp. To genotype the *rbx2* knockout blastocysts/pups (rbx2KO), we used the following primers (Fig. 1B, arrowheads): primer C-2, 5'-gcctgtgcaacatgaaaccc-3'; primer Wt-2, 5'-ATCGGGCCTCATATAGCCCA-3'; primer KO, 5 '-ATCTCCCCAGCCCCTAACAT-3'. Primer C-2 and primer WT-2 generated an amplicon in the wild-type allele of 254 bp, and primer C-2 and primer KO produced an amplicon in the mutant allele of 405 bp. Adult animals (AD) are 60 to 90 days old.

Blastocyst Collection

Blastocysts were collected as explained elsewhere (Hofker and van Deursen, 2011). Briefly, heterozygous *cul5GT* or heterozygous *rbx2*KO mice were mated overnight. The morning when a vaginal plug was found was considered E0.5 and the female was separated. After 3 days, females were euthanized and both uteri carefully dissected. Blastocysts were collected by flushing the uterus lumen twice with 100 μl of DMEM media (Thermo Fisher Scientific). Blastocysts were collected using a pulled capillary and digested with proteinase K before genotyping.

X-Gal Staining

For in toto staining, embryos were dissected at E7, E9, and E11 and submerged in a 1:1 solution of formalin 3.65% (Protocols, MI) and PBS (0.1 M phosphate, 0.15 M NaCl) for 2 hr at 4 °C. After fixation, embryos were washed twice with PBS, permeabilized for 20 min with 0.02% IGEPAL CA 630 (Sigma), and incubated overnight at 37 °C with staining solution (1 mg/ml X-Gal [5-bromo-4-chloro-3-indolyl-ß-Dgalactopyranoside], 5 mM potassium ferricyanide, 5 mM potassium ferrocyanide, 2 mM MgCl2, 2.5% DMSO, 0,02% IGEPAL CA 630 in PBS). The next day, embryos were washed twice with PBS and post-fixed with formalin. For samples of E14-P5 embryos, brains were carefully dissected out,

Author Manuscript Author Manuscript Author Manuscript Author Manuscript

fixed as previously described, and cryoprotected with 30% sucrose in PBS overnight at 4 °C. The next day, brains were frozen in optimal cutting temperature (OCT) compound and cryosectioned at 14 μm. Brain slices were permeabilized and stained as in the in toto stainings. For adult samples, brains were fixed by intracardiac perfusion with 1.82% formalin and processed as described. At every age analyzed, wild-type littermates were stained in parallel and no staining was detected. Microphotographs were taken using an Axio Observer.Z1 ZEISS microscope and assembled by the AxioVision Imaging software (ZEISS). In toto pictures were taken using a Leica DFC290 camera. Images were processed using Adobe Photoshop software and figures were mounted in Adobe Illustrator.

Immunofluorescence

Adult (2-month-old) CD1 mice were transcardially perfused with 4% paraformaldehyde and embedded in paraffin; 8-μm sagittal sections were obtained and deparaffinized. Samples were treated with 10 mM sodium citrate (pH 6) in a food steamer for 40 min, washed once in PBS, and blocked with a PBS, 0.5% Triton X, and 5% nonfat milk solution for 2 hr at room temperature. Next, samples were incubated in blocking solution with Cul5 (Rockland #100–401-A05, 1:50) or Rbx2 (Abcam #ab181986, 1:50) antibodies for 72 hr at 4 °C. Costaining of Cul5 and ß-Gal (Abcam #ab9361, 1:200) was performed in the same conditions. Alexa488- and Alexa568-labelled secondary antibodies (Life Technologies, 1:200) in blocking solution were incubated for 24 hr and DAPI was used as counterstaining. Microphotographs were taken using a Dragonfly microscopy system (Andor). Images were processed using Fiji software (images were stitched using the plugin developed by Preibisch et al.) (Preibisch et al., 2009), and figures were mounted in Adobe Illustrator.

Statistics

Statistical analyses were performed with Excel (Microsoft). Litters from *cul5GT* and rbx2KO intercrossings were genotyped as described, and deviations from a 1:2:1 segregation ratio were tested at the indicated ages using the Chi-square (χ^2) test. *P* values were indicated in each case.

Supplementary Material

Refer to Web version on PubMed Central for supplementary material.

Acknowledgments

This work was supported by the University of California start-up funds to S.S. and grants R01 NS080194 and R01 GM109463 from the US Public Health Service to J.A.C. The Fred Hutchinson Comparative Medicine and Transgenic facilities are supported by P30 CA015704. We thank Reice D. James and Nanyang Jiang for expert technical assistance.

References

Arai T, Kasper JS, Skaar JR, Ali SH, Takahashi C, DeCaprio JA. 2003 Targeted disruption of p185/Cul7 gene results in abnormal vascular morphogenesis. Proc Natl Acad Sci U S A 100: 9855–9860. [PubMed: 12904573]

Bayer SA. 1983 3H-thymidine-radiographic studies of neurogenesis in the rat olfactory bulb. Exp Brain Res 50:329–340. [PubMed: 6641865]

Author Manuscript Author Manuscript Author Manuscript Author Manuscript

Ceremuga TE, Yao XL, McCabe JT. 2001 Vasopressin-activated calcium-mobilizing (VACM-1) receptor mRNA is present in peripheral organs and the central nervous system of the laboratory rat. Endocr Res 27:433–445. [PubMed: 11794467]

Ceremuga TE, Yao XL, McCabe JT. 2003 Cullin-5 is ubiquitous in the rat brain. Neurosci Lett 345:121–125. [PubMed: 12821186]

Dealy MJ, Nguyen KV, Lo J, Gstaiger M, Krek W, Elson D, Arbeit J, Kipreos ET, Johnson RS. 1999 Loss of Cul1 results in early embryonic lethality and dysregulation of cyclin E. Nat Genet 23:245–248. [PubMed: 10508527]

Dentice M, Bandyopadhyay A, Gereben B, Callebaut I,Christoffolete MA, Kim bW, Nissim S, Mornon Jp, Zavacki AM, Zeold A, Capelo LP, Curcio-Morelli C, Ribeiro, Harney JW, Tabin CJ, Bianco AC. 2005 The Hedgehog-inducible ubiquitin ligase subunit WSB-1 modulates thyroid hormone activation and PTHrP secretion in the developing growth plate. Nat Cell Biol 7: 698–705. [PubMed: 15965468]

Fairchild CL, Hino K, Han JS, Miltner AM, Peinado Allina G, Brown CE, Burns ME, La Torre A, Simo S. 2018 RBX2 maintains final retinal cell position in a DAB1-dependent and -independent fashion. Development 145:pii dev155283.

Farley FW, Soriano P, Steffen LS, Dymecki SM. 2000 Widespread recombinase expression using FLpeR (flipper) mice. Genesis 28: 106–110. [PubMed: 11105051]

Feng L, Allen NS, Simo S, Cooper JA. 2007 Cullin 5 regulates Dab1 protein levels and neuron positioning during cortical development. Genes Dev 21:2717–2730. [PubMed: 17974915]

Hofker MH, van Deursen JM. 2011 Transgenic Mouse Methods and Protocols, Second Edition 693:1–352.

Huang DT, Ayrault O, Hunt HW, Taherbhoy AM, Duda DM, Scott DC, Borg LA, Neale G, Murray PJ, Roussel MF, Schulman BA. 2009 E2-RING expansion of the NEDD8 cascade confers specificity to cullin modification. Mol Cell 33:483–495. [PubMed: 19250909]

Jiang Y, He X, Howe PH. 2012 Disabled-2 (Dab2) inhibits Wnt/-beta-catenin signalling by binding LRP6 and promoting its internalization through clathrin. EMBO J 31:2336–2349. [PubMed: 22491013]

Kamura T, Burian D, Yan Q, Schmidt SL, Lane WS, Querido E, Branton PE, Shilatifard A, Conaway RC, Conaway JW. 2001 Muf1, a novel Elongin BC-interacting leucine-rich repeat protein that can assemble with Cul5 and Rbx1 to reconstitute a ubiquitin ligase. J Biol Chem 276:29748–29753. [PubMed: 11384984]

Kelsall IR, Duda DM, Olszewski JL, Hofmann K, Knebel A, Langevin F, Wood N, Wightman M, Schulman BA, Alpi AF. 2013 TRIAD1 and HHARI bind to and are activated by distinct neddylated Cullin-RING ligase complexes. EMBO J 32:2848–2860. [PubMed: 24076655]

Khalaf-Nazzal R, Francis F. 2013 Hippocampal development - old and new findings. Neuroscience 248:225–242. [PubMed: 23756184]

Kopanja D, Roy N, Stoyanova T, Hess RA, Bagchi S, Raychaudhuri P. 2011 Cul4A is essential for spermatogenesis and male fertility. Dev Biol 352:278–287. [PubMed: 21291880]

Laszlo GS, Cooper JA. 2009 Restriction of Src activity by Cullin-5. Curr Biol 19:157–162. [PubMed: 19147357]

Li B, Ruiz JC, Chun KT. 2002 CUL-4A is critical for early embryonic development. Mol Cell Biol 22:4997–5005. [PubMed: 12077329]

Lledo PM, Merkle FT, Alvarez-Buylla A. 2008 Origin and function of olfactory bulb interneuron diversity. Trends Neurosci 31:392–400. [PubMed: 18603310]

Mahrour N, Redwine WB, Florens L, Swanson SK, Martin-Brown S, Bradford WD, Staehling-Hampton K, Washburn MP, Conaway RC, Conaway JW. 2008 Characterization of Cullin-box sequences that direct recruitment of Cul2-Rbx1 and Cul5-Rbx2 modules to Elongin BC-based ubiquitin ligases. J Biol Chem 283:8005–8013. [PubMed: 18187417]

Moon UY, Park JY, Park R, Cho JY, Hughes LJ, McKenna J 3rd, Goetzl L, Cho SH, Crino PB, Gambello MJ, Kim S. 2015 Impaired Reelin-Dab1 Signaling Contributes to Neuronal Migration Deficits of Tuberous Sclerosis Complex. Cell Rep 12:965–978. [PubMed: 26235615]

Okumura F, Joo-Okumura A, Nakatsukasa K, Kamura T. 2016 The role of cullin 5-containing ubiquitin ligases. Cell Div 11:1. [PubMed: 27030794]

Author Manuscript Author Manuscript Author Manuscript Author Manuscript

Onel M, Sumbul F, Liu J, Nussinov R, Haliloglu T. 2017 Cullin neddylation may allosterically tune polyubiquitin chain length and topology. Biochem J 474:781–795. [PubMed: 28082425]

Petroski MD, Deshaies RJ. 2005 Function and regulation of cullin-RING ubiquitin ligases. Nat Rev Mol Cell Biol 6:9–20. [PubMed: 15688063]

Preibisch S, Saalfeld S, Tomancak P. 2009 Globally optimal stitching of tiled 3D microscopic image acquisitions. Bioinformatics 25: 1463–1465. [PubMed: 19346324]

Sarikas A, Hartmann T, Pan ZQ. 2011 The cullin protein family. Genome Biol 12:220. [PubMed: 21554755]

Sasagawa Y, Sato S, Ogura T, Higashitani A. 2007 C. elegans RBX-2-CUL-5- and RBX-1-CUL-2-based complexes are redun-dant for oogenesis and activation of the mAp kinase MPK-1. FEBS Lett 581:145–150. [PubMed: 17184777]

Saunders A, Macosko EZ, Wysoker A, Goldman M, Krienen FM, de Rivera H, Bien E, Baum M, Bortolin L, Wang S, Goeva A, Nemesh J, Kamitaki N, Brumbaugh S, Kulp D, McCarroll SA. 2018 Molecular Diversity and Specializations among the Cells of the Adult Mouse Brain. Cell 174:1015–1030. [PubMed: 30096299]

Simo S, Cooper JA. 2013 Rbx2 regulates neuronal migration through different cullin 5-RING ligase adaptors. Dev Cell 27: 399–411. [PubMed: 24210661]

Simo S, Jossin Y, Cooper JA. 2010 Cullin 5 regulates cortical layering by modulating the speed and duration of Dab1-dependent neuronal migration. J Neurosci 30:5668–5676. [PubMed: 20410119]

Singer JD, Gurian-West M, Clurman B, Roberts JM. 1999 Cullin-3 targets cyclin E for ubiquitination and controls S phase in mammalian cells. Genes Dev 13:2375–2387. [PubMed: 10500095]

Skarnes WC, Rosen B, West AP, Koutsourakis M, Bushell W, Iyer V, Mujica AO, Thomas M, Harrow J, Cox T, Jackson D, Severin J, Biggs P, Fu J, Nefedov M, de Jong PJ, Stewart AF, Bradley A. 2011 A conditional knockout resource for the genome-wide study of mouse gene function. Nature 474: 337–342. [PubMed: 21677750]

Tallquist MD, Soriano P. 2000 Epiblast-restricted Cre expression in MORE mice: a tool to distinguish embryonic vs. extra-embryonic gene function. Genesis 26:113–115. [PubMed: 10686601]

Tan M, Zhao Y, Kim SJ, Liu M, Jia L, Saunders TL, Zhu Y, Sun Y. 2012 SAG/RBX2/ROC2 E3 ubiquitin ligase is essential for vascu-lar and neural development by targeting NF1 for degradation. Dev Cell 21:1062–1076.

Teckchandani A, Laszlo GS, Simo S, Shah K, Pilling C, Strait AA, Cooper JA. 2014 Cullin 5 destabilizes Cas to inhibit Src-dependent cell transformation. J Cell Sci 127:509–520. [PubMed: 24284072]

Torres-Reveron J, Friedlander MJ. 2007 Properties of persis-tent postnatal cortical subplate neurons. J Neurosci 27: 9962–9974. [PubMed: 17855610]

Wang X, Wang X, Wang W, Zhang J, Wang J, Wang C, Lv M, Zuo T, Liu D, Zhang H, Wu J, Yu B, Kong W, Wu H, Yu X. 2015 Both Rbx1 and Rbx2 exhibit a functional role in the HIV-1 Vif-Cullin5 E3 ligase complex in vitro. Biochem Biophys Res Commun 461: 624629.

Wang Y, Penfold S, Tang X, Hattori N, Riley P, Harper JW, Cross JC, Tyers M. 1999 Deletion of the Cul1 gene in mice causes arrest in early embryogenesis and accumulation of cyclin E. Curr Biol 9:1191–1194. [PubMed: 10531039]

Willis AN, Dean SE, Habbouche JA, Kempers BT, Ludwig ML, Sayfie AD, Lewis SP, Harrier S, DeBruine ZJ, Garrett R, Burnatowska-Hledin MA. 2017 Nuclear localization signal sequence is required for VACM-1/CUL5-dependent regulation of cellular growth. Cell Tissue Res 368:105–114. [PubMed: 27834018]

Zeisel A, Hochgerner H, Lonnerberg P, Johnsson A, Memic F, van der Zwan J, Haring M, Braun E, Borm LE, La Manno G, Codeluppi S, Furlan A, Lee K, Skene N, Harris KD, Hjerling-Leffler J, Arenas E, Ernfors P, Marklund U, Linnarsson S. 2018 Molecular Architecture of the Mouse Nervous System. Cell 174:999–1014. [PubMed: 30096314]

Author Manuscript Author Manuscript Author Manuscript Author Manuscript

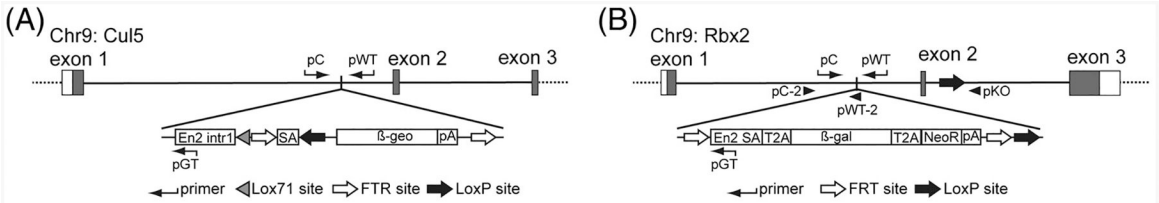

(C)

	cul5 +/+	*cul5* GT/+	*cul5* GT/GT	Total	χ^2
P0	10	30	0	40	0.00055
E3.5	14	32	0	46	0.00041
Total	24	62	0	86	2.78×10^{-7}

(D)

	rbx2 +/+	*rbx2* +/-	*rbx2* -/-	Total	χ^2
P0	13	23	0	36	0.00228
E3.5	14	55	6	75	0.00012
Total	27	78	6	111	2.05×10^{-6}

Fig. 1.

Disruption of *cul5* and *rbx2* causes embryonic lethality at different developmental stages. Diagram of *cul5*GT (**A**) and rbx2GT (**B**) alleles indicating the LacZ cassette insertion in the first intron in both genes. Notice that whereas cul5GT and rbx2GT generate null alleles, rbx2GT can be converted to a conditional allele (rbx2fl) via FLPe recombination and to a knockout allele (rbx2KO) via CRE recombination. White boxes in exons indicate untranslated regions and gray boxes indicate coding sequences. Genotyping primers and their relative positions are indicated. Detailed explanation of genotyping strategy can be found in the Material and Methods section. **C**: No homozygous cul5GT embryos were collected from n = 6 litters at E3.5 and n = 5 litters analyzed at P0. On the contrary, homozygous rbx2KO embryos were collected at E3.5 (n = 15 litters) but failed to survive until birth (n = 6 litters) (**D**). The number of embryos obtained per genotype and age is indicated in each case. Differences from expected Mendelian ratio were tested using the Chi-square test (χ^2), and P values are indicated in each case. ß-gal, beta-galactosidase; ß-geo, beta-galactosidase + Neomycin resistance gene; Chr9, chromosome 9; En2 intr1, partial Engrailed 2 Intron 1; En2 SA, Engrail 2 splicing acceptor; NeoR, Neomycin-resistance gene; pA, polyadenylation site; SA, splicing acceptor; T2A, thosea asigna virus 2A peptide.

Author Manuscript Author Manuscript Author Manuscript Author Manuscript

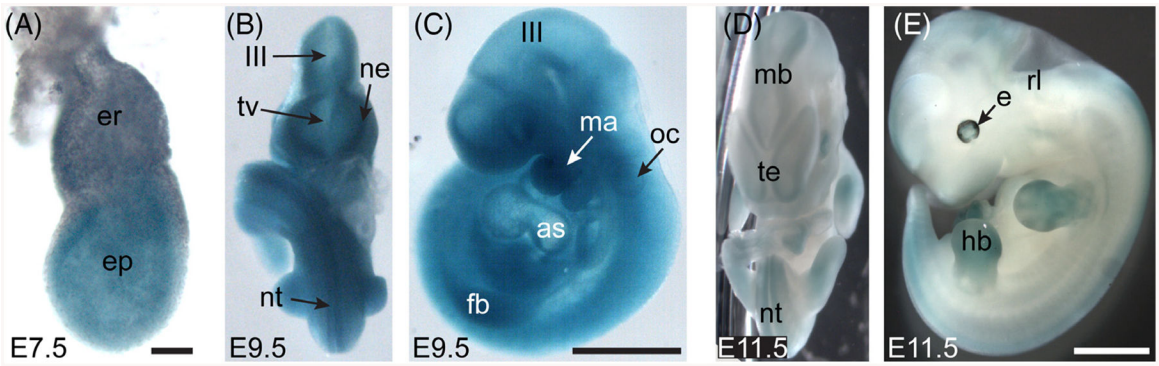

Fig. 2.

Expression of *cul5* in whole mouse embryo during mid-gestation. In toto LacZ staining at E7.5 (**A**), E9.5 (**B**, frontal view; **C**, lateral view), and E11.5 (**D**, frontal view; **E**, lateral view). *cul5* was ubiquitously expressed in the embryo proper at E7.5 (A). By E9.5, its expression was increasingly restricted to the CNS and developing limbs (B-E). as, aortic sac; er, extraembryonic body; e, eye; ep, embryo proper; fb, left forelimb bud; hb, left hindlimb bud; III, third ventricle; ma, mandibular compartment of first branchial arch; mb, midbrain; ne, neuroepithelium; nt, neural tube; oc, otocyst; rb, rhombic lip; tv, telencephalic vesicle; te, telencephalon. Scale bar A = 50 μm. Scale bars B,C = 500 μm. Scale bars D,E = 1 mm.

Author Manuscript Author Manuscript Author Manuscript Author Manuscript

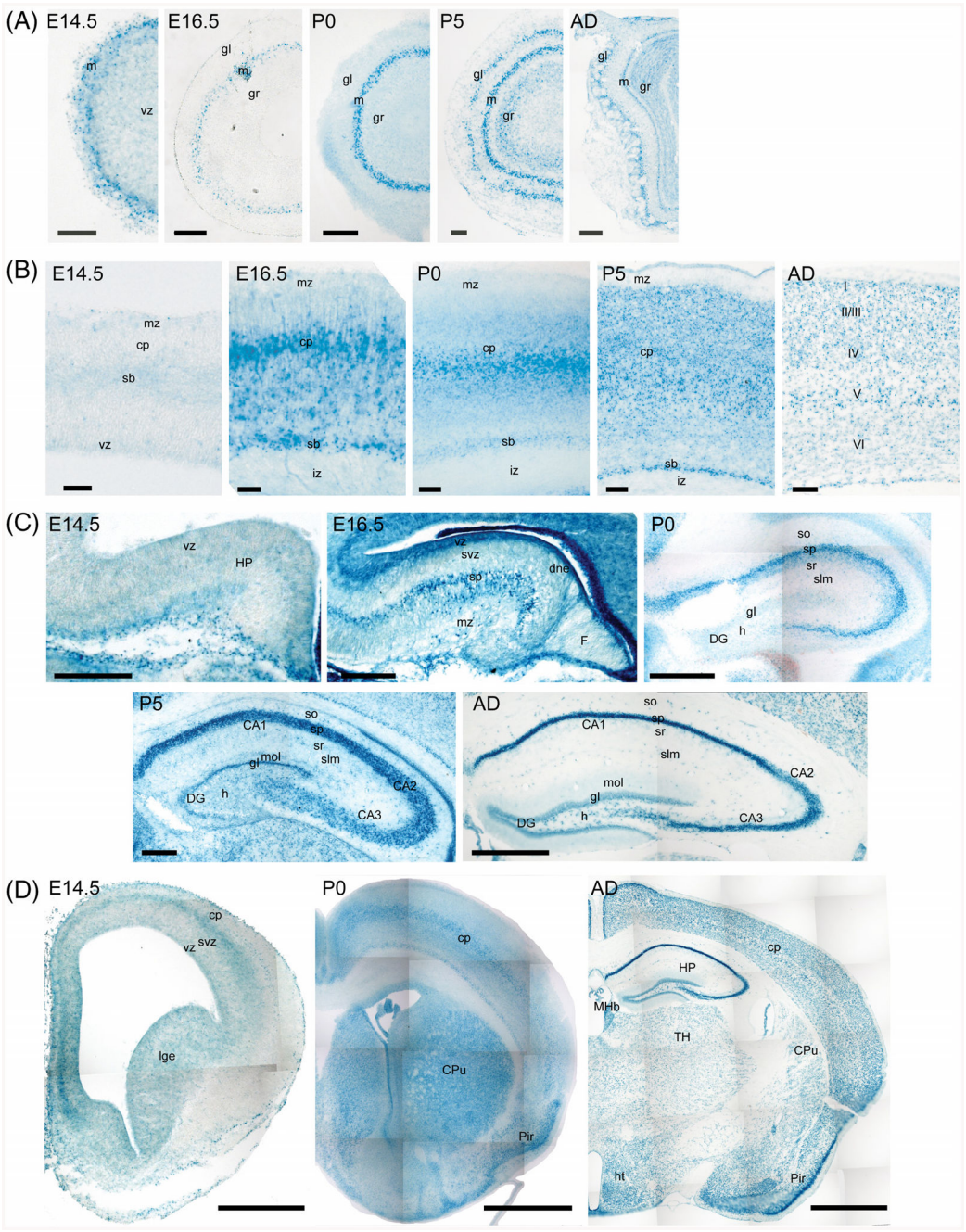

Fig. 3.

Expression of *cul5* in the forebrain during development and in the adult. Ontogenic analysis of *cul5* expression using x-Gal staining in the olfactory bulb (**A**), neocortex (**B**), hippocampus (**C**), and forebrain (**D**) of heterozygous cul5GT animals. *cul5* was strongly expressed in several areas of the forebrain, including the mitral layer in the olfactory bulb (A) and the neocortex (B). Whereas pyramidal cells of the hippocampus were positive for LacZ during development and in the adult, granule cells in the dentate gyrus expressed *cul5* only in postnatal stages. CA1-CA3, Cornu Ammonis 1–3; cp, cortical plate; CPu, caudate-putamen; DG, dentate gyrus; dne, dentate neuroepithelium; F, fimbria; gl, glomerular layer;

Author Manuscript Author Manuscript Author Manuscript Author Manuscript

gr, granular layer; h, hilus; HP, hippocampus; ht, hypothalamus; I-VI, layer I-VI of the neocortex; iz, intermediate zone; lge, lateral ganglionic eminence; m, mitral layer; MHb, medial habenula; mol, molecular layer of the hippocampus; mz, marginal zone; Pir, piriform cortex; sb, subplate; slm, stratum lacunosum moleculare; so, stratum oriens; sp, stratum pyramidale; sr, stratum radiatum; svz, subventricular zone; vz, ventricular zone. Scale bars A,B = 50 μm. Scale bar C = 200 μm. Scale bar E = 500 μm.

Author Manuscript Author Manuscript Author Manuscript Author Manuscript

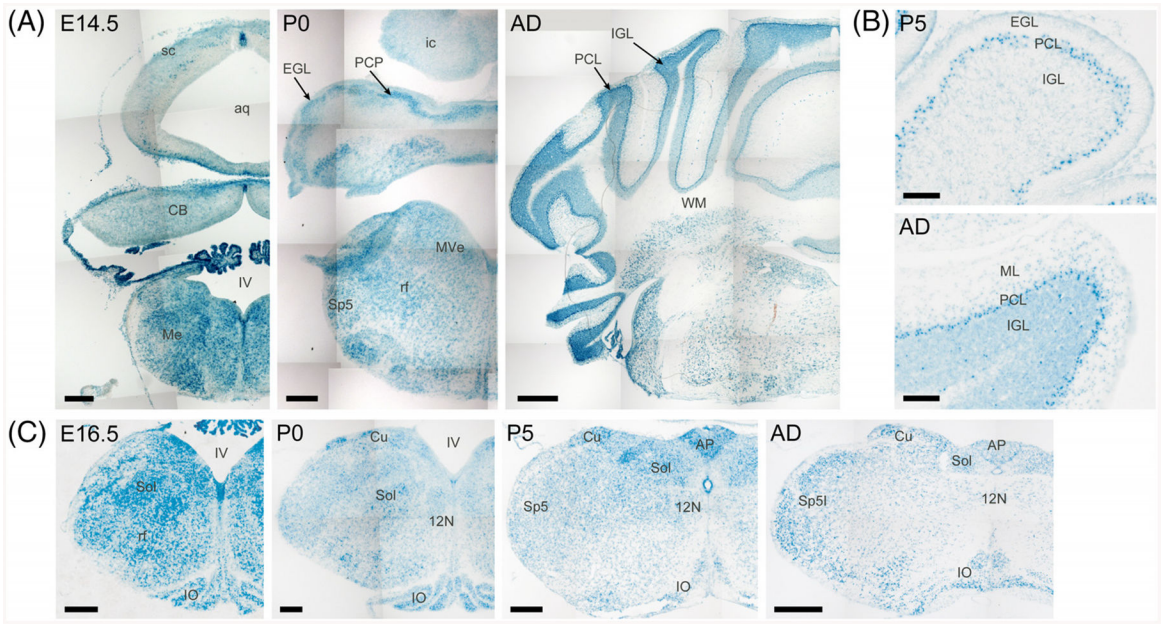

Fig. 4.

Expression of *cul5* in the diencephalon and medulla. *cul5* was strongly expressed in the medulla at early embryonic stages (**A**, E14.5; **C**, E16.5) and its expression decreased at later time points (A,C). Expression of *cul5* was strong in Purkinje cells during development and in the adult (A). High-power images (**B**) showed that *cul5* was also expressed in the granule cells of the cerebellum, particularly in the adult (AD). AP, area postrema; aq, aqueduct; CB, cerebellum; Cu, cuneate nucleus; EGL, external granular layer; ic, inferior colliculus; IGL, internal granular layer; IO, inferior olive; IV, fourth ventricle; Me, medulla; ML, molecular layer; MVe, medial vestibular nucleus; PCP, Purkinje cell plate; PCL, Purkinje cell layer; rf, reticular formation; sc, superior colliculus; Sol, solitary tract nucleus; Sp5, spinal trigeminal nucleus; WM, white matter; 12N, hypoglossal nerve. Scale bars = 500 μm.

Author Manuscript Author Manuscript Author Manuscript Author Manuscript

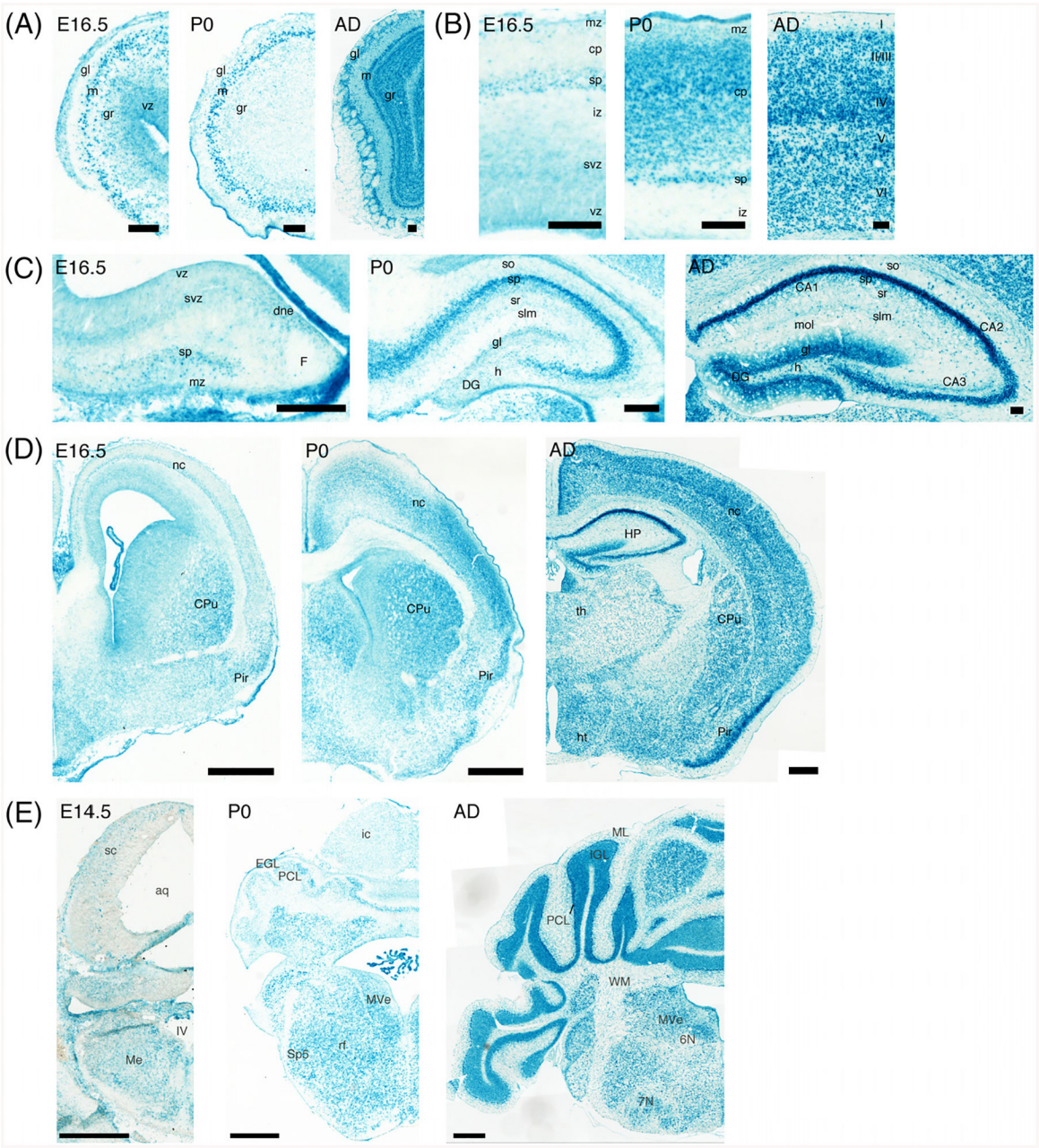

Fig. 5.

Expression of *rbx2* during development and in the adult brain. *rbx2* expression parallels *cux5* expression in all the areas analyzed. In the olfactory bulb, *rbx2* was strongly expressed in the mitral layer at all ages analyzed, and expression of rbx2 was detected in granule cells at postnatal stages only (**A**). *rbx2* expression in the neocortex was detected in proliferative zones as well as in somatic areas (B) (E16.5 and P0). In the adult neocortex, strong LacZ staining was observed in all cortical layers (AD). Similar to *cu/5, rbx2* was detected in proliferative areas of the hippocampus and in the stratum pyramidale at early stages (**C**) (E16.5). LacZ signal was detected in the dentate gyrus starting at postnatal stages and reaching maximum expression in the adult (P0 and AD). Comparative analysis of *rbx2*

Author Manuscript Author Manuscript Author Manuscript Author Manuscript

expression in the forebrain indicated that *rbx2* was ubiquitously expressed during development and in the adult (**D**). In the hindbrain, *rbx2* expression was detected principally in Purkinje cells, deep cerebellar nuclei, and medulla (E14.5 and P0). In the adult cerebellum, a strong LacZ staining was observed in Purkinje cells, but especially in granule cells of the internal granular layer, similar to *cu/5*. th, thalamus; 6N, abducens nucleus; 7N, facial nucleus. Scale bars A,C = 100 μm. Scale bars D,E = 500 μm.

Author Manuscript Author Manuscript Author Manuscript Author Manuscript

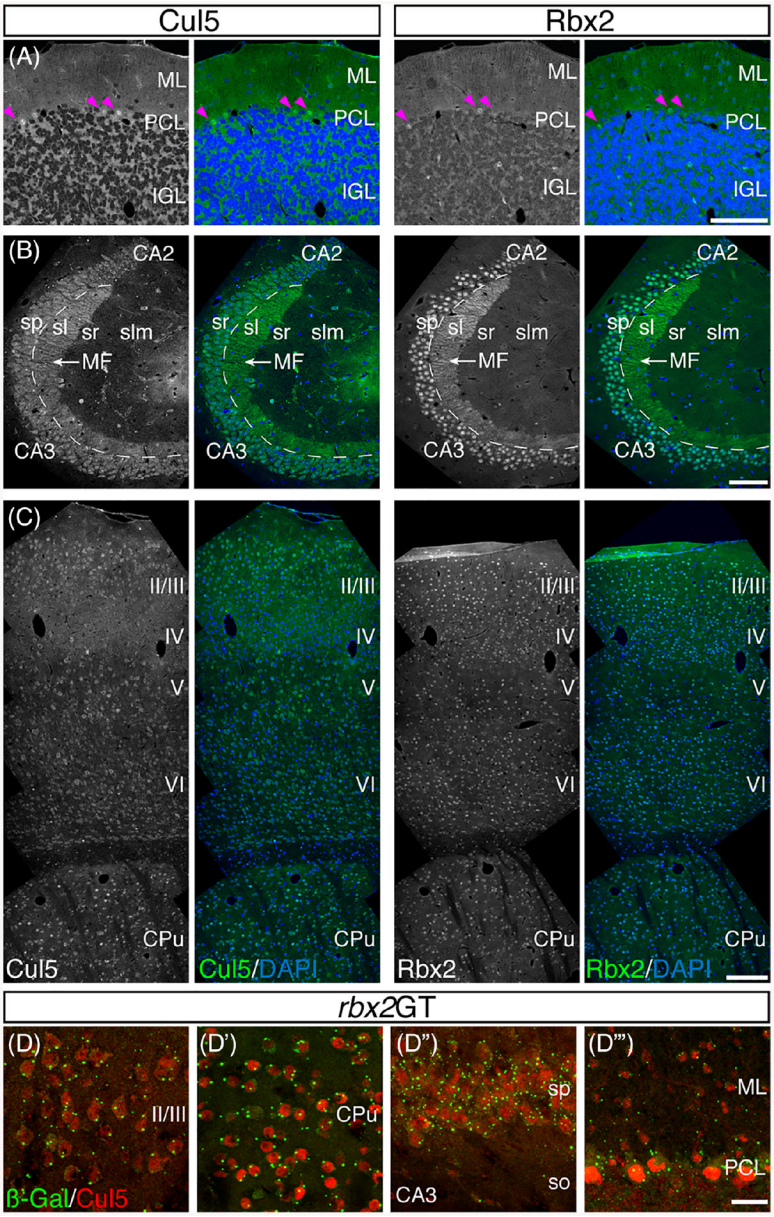

Fig. 6.

Co-expression of Cul5 and Rbx2 in the adult brain. Comparative analysis of Cul5 and Rbx2 by immunofluorescence in consecutive wild-type adult brain sections. In the cerebellum, both Cul5 and Rbx2 were detected in the nuclei of Purkinje cells (purple arrowheads) and broadly distributed in the internal granular layer (**A**). In the hippocampus, Cul5 was detected principally in the cytoplasm of the pyramidal cells of the cornu ammonis and in mossy fibers. Rbx2 was detected in the nuclei of pyramidal cells and in mossy fibers (**B**). In the neocortical neurons, Cul5 was detected in the cytoplasm and Rbx2 in the nucleus. On the contrary, in the caudate-putamen, both Cul5 and Rbx2 have a nuclear localization. **D-D'"**: Immunofluorescence against ß-galactosidase and Cul5 in adult rbx2GT tissue shows ubiquitous colocalization, including the neocortex (D), caudate-putamen (D"), hippocampus

(D“), and cerebellum (D”’). MF, mossy fibers; sl, stratum lucidum. Scale bars A,B = 100 μm. Scale bar C = 500 μm. Scale bar D = 25 μm.

Author Manuscript Author Manuscript Author Manuscript Author Manuscript